Parallel-Oriented Fibrogenesis of a β-Sheet Forming Peptide on Supported Lipid Bilayers

ARTICLE *in* THE JOURNAL OF PHYSICAL CHEMISTRY B · JULY 2008

Impact Factor: 3.3 · DOI: 10.1021/jp802424h

Parallel-Oriented Fibrogenesis of a β-Sheet Forming Peptide on Supported Lipid Bilayers

Lan Zhang, Jian Zhong, Lixin Huang, Lijun Wang, Yuankai Hong, and Yinlin Sha*

Single-Molecule and Nanobiology Laboratory, Department of Biophysics, School of Basic Medical Sciences, Biomed-X Center, and Center for Protein Science, Peking University, Beijing 100083, China

Received: March 19, 2008; Revised Manuscript Received: May 12, 2008

Peptide self-assembly on substrates is currently an intensively studied topic that provides a promising strategy for fabrication of soft materials and is also important for revealing the surface chemistry of amyloidogenic proteins that aggregate on cell membranes. We investigated the fibrogenesis of a β-sheet forming peptide $A\beta_{26-35}$ on supported lipid bilayers (SLBs) by in situ atomic force microscopy (AFM), circular dichroism (CD), and attenuated total reflectance Fourier transform infrared (ATR-FTIR) spectroscopy. The results show that the $A\beta_{26-35}$ nanofilaments' growth is oriented to a specific direction and formed a highly ordered, large-scale, parallel-oriented surface pattern on membranes. The parallel-oriented fibrogenesis of $A\beta_{26-35}$ was able to occur on different lipid membranes rather than on solid substrates. It implies that the parallel-oriented fibrogenesis was associated with the distinct properties of lipid membranes, such as the fluid nature of lipid molecules on membranes. The membrane fluidity may allow the peptide assemblies to float at the water−membrane interface and easily orient to an energetically favorable state. These results provide an insight into the surface chemistry of peptide self-assembly on lipid membranes and highlight a possible way to fabricate supramolecular architectures on the surface of soft materials.

Introduction

Peptide self-assembly is a spontaneous organization of peptide molecules into ordered supramolecular structures, such as fibrils, vesicles, and tubes. It allows one to define the ultimate material properties by designing the peptide molecules, namely, the building blocks.[1–7] The peptide self-assembly has been a promising bottom-up strategy to develop soft materials with diverse properties, available for potential biological applications.[8–10] For instance, Zhang and his co-workers[11,12] have reported that short peptides self-assembled into stable hydrogels can be applied in tissue engineering, such as cartilage repair, promotion of nerve cell growth, and brain tissue restoration. Remarkably, fibrogenesis of β-structural proteins/peptides is also an important pathological event involved in protein conformational diseases, such as amyloid β-protein (Aβ) in Alzheimer's disease, PrP in Prion diseases, and α-synuclein in Parkinson disease.[13,14] Therefore, peptide self-assembly studies will not only facilitate the production of special nanostructural biomaterials, but also provide insights into the nature underlying the abnormal fibrogenesis in protein conformational diseases.

In recent years, several amyloidogenic proteins/peptides have been reported to self-assemble into nanowire arrays on inorganic crystals, such as mica and HOPG (highly oriented pyrolytic graphite), in which the inorganic crystals act as the templates to assist the peptide fibrogenesis along their surface structural lattice (termed template-assisted epitaxial growth, TAEG), and significantly affect the dynamics of peptide fibrogensis.[15–19] In addition to the "hard" inorganic crystals, there is a large class of "soft" materials available for use, which possess many distinct properties and functions. For instance, cell membranes, regular two-dimensional structures assembled predominately by lipid molecules, play many important roles in terms of physiology and pathology. Recent experiments have demonstrated that cell membranes are involved in the abnormal protein aggregation in protein conformational diseases, such as the Aβ fibrogenesis in Alzheimer's disease.[20,21] Therefore, studies of peptide self-assembly on lipid membranes are important for investigation of the pathological protein fibrogenesis in protein conformational diseases, and also offer a fundamentally scientific opportunity to fabricate supramolecular architectures on the surface of soft materials via peptide self-assembly.

The lipid molecule POPC (1-palmitoyl-2-oleoyl-*sn*-glycero-3-phosphocholine) is one of the important constituents of cell membranes and is generally used to study membrane structures, properties, and related interactions because its low melting point results in the fluid L-phase at room temperature. $A\beta_{26-35}$ is a key fragment of Aβ in Alzheimer's disease and has been used as one of the substitutes of Aβ for structural and pathologic studies.[22,23] It possesses strong propensities of β-sheet formation and the consequent fibrogenesis under specific conditions. In this paper, we studied the $A\beta_{26-35}$ fibrogenesis on mica-supported lipid bilayers (SLBs) of POPC by in situ atomic force microscopy (AFM), circular dichroism (CD), and Fourier transform infrared (FTIR), to reveal the physicochemical characteristics of $A\beta_{26-35}$ self-assembly on lipid membranes.

Experimental Methods

Peptides. $A\beta_{26-35}$ ($H_2N-SNKGAIIGLM-CONH_2$) was prepared by a standard solid-phase peptide synthetic strategy of Fmoc chemistry[24] and was purified by HPLC and confirmed by using matrix-assisted laser desorption ionization time-of-flight mass spectrometry (MALDI-TOF MS; $[M+H]^+$: obsd, 1002.3; calcd, 1002.0). The purified peptide powder was kept at −20 °C prior to use.

SLB Preparation. Supported lipid bilayers (SLBs) were prepared using the vesicle fusion method.[25–27] Briefly, the lipid was dissolved in chloroform/methanol (2:1, v/v) and then dried in a rotary evaporator and kept under high vacuum overnight. An appropriate amount of HBS1 buffer (50 mM Hepes, 100

* To whom correspondence should be addressed. Tel./Fax: +86-10-82801278. E-mail: shyl@hsc.pku.edu.cn.

10.1021/jp802424h CCC: $40.75
Published on Web 07/02/2008

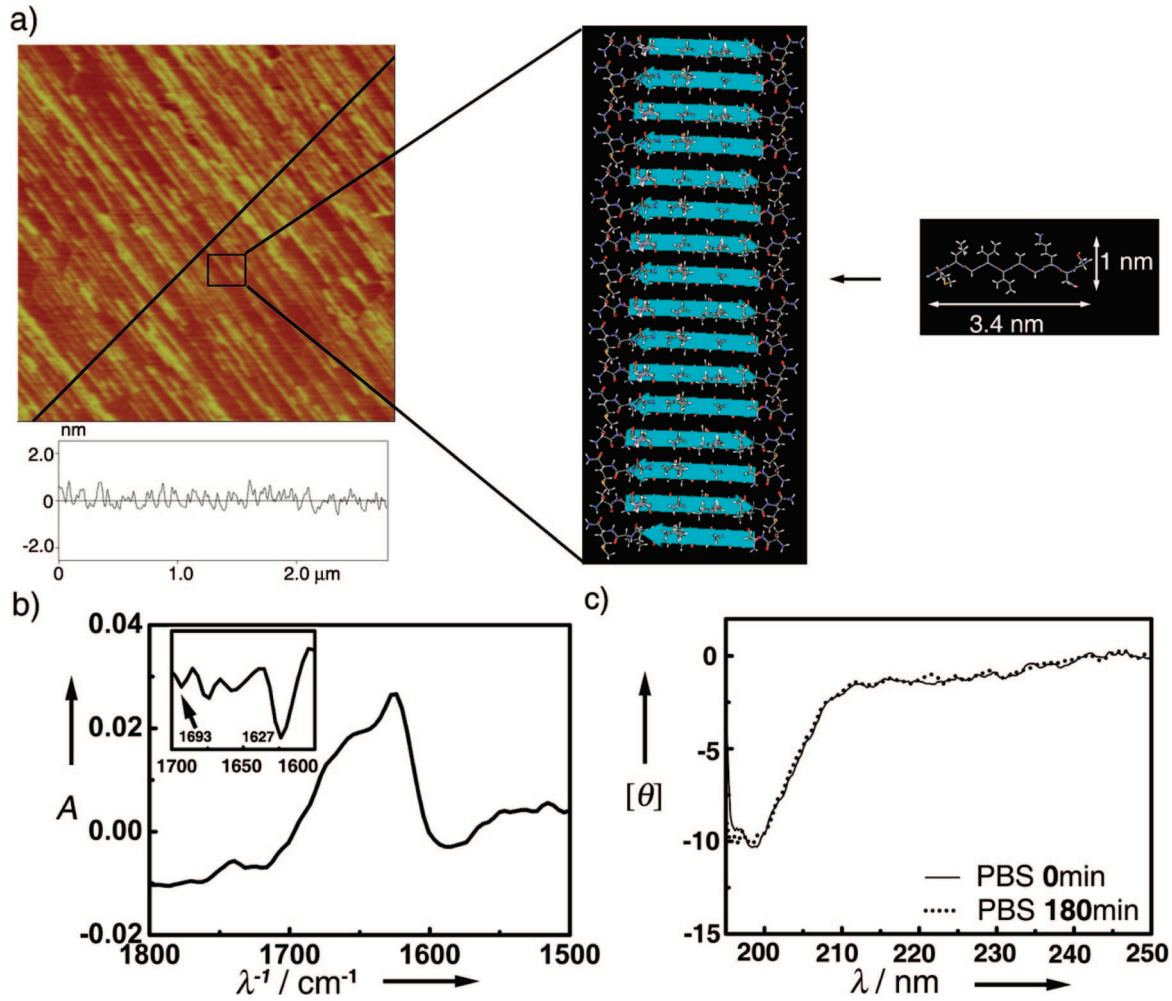

Figure 1. (a) Representative AFM image of Aβ_{26-35} nanofilaments on the POPC SLB, and the molecular model of Aβ_{26-35} with an extended structure and its single β-sheet alignment in an antiparallel fashion. The section analysis is shown in the bottom. Image size: 2 × 2 μm. *Z* scale: 5 nm. (b) Solid phase ATR-FTIR spectra of Aβ_{26-35} on the POPC SLB. The inset shows the derivative analysis that displays a strong absorption peak at about 1627 cm^{-1} and a weak band around 1693 cm^{-1} indicating an antiparallel β-sheet conformation. (c) CD spectra of Aβ_{26-35} incubated for 0 and 180 min respectively present a negative absorption at about 198 nm, a typical characteristic of random coil.

mM NaCl, and 2 mM $CaCl_2$, pH 7.4) was added to the sample to hydrate the lipid, and then the sample was shaken vigorously to get MLVs (multilamellar vesicles). LUVs (large unilamellar vesicles) were prepared by extrusion of the MLVs through a 0.1 μm polycarbonate membrane (Avanti Polar Lipids) at 65 °C. The LUV suspension was pipetted onto the freshly cleaved mica and incubated at 70 °C for 2 h in a water bath. The bilayers were slowly cooled to room temperature at ambient conditions and then carefully rinsed with HBS2 buffer (50 mM Hepes, 100 mM NaCl, pH 7.4) to remove the excess LUVs and the loosely adsorbed bilayers. In the experiments, the prepared SLBs were intact before the peptide treatment and can be stable for several days at room temperature.

In Situ AFM Experiments. In situ AFM experiments were performed on a multimode atomic force microscope with a Nanoscope IV controller and equipped with an EV scanner (Veeco Instruments Inc.). Scans were carried out by using the sharpened OTR8 cantilevers with a nominal spring constant of 0.15 N/m. The cantilever oscillation was tuned to a frequency of 7−10 kHz, and the drive amplitude was adjusted to get the root mean square (rms) amplitude of about 1.0−2.0 V. The scan rate was typically set at 1.49 Hz. The Aβ_{26-35} solution was injected into the imaging liquid to make a final concentration of 50 μM and imaged immediately. A 20 μL aliquot of HBS2 buffer was injected into the imaging liquid every 2 h to make up the evaporated liquid. The scanning was performed at room temperature. The AFM imaging of Aβ_{26-35} fibrogenesis on glass (Fisher Scientific Co.) and siliconized glass (Hampton Research) was carried out under the same conditions. All images were captured as 512 × 512 pixel scans and were flattened and plane-fitted by Nanoscope III software (Ver. 5.12r2, Veeco) before the data analysis.

CD Experiments. CD spectra were recorded on a JASCO spectropolarimeter of J-180 at a peptide concentration of 50 μM in 50 mM phosphate-buffered saline (PBS), pH 7.4. For solution CD spectra, a cell with 1.0 mm path length was used. The spectra were scanned between 190 and 250 nm with a 0.2 nm step resolution. Three scans were averaged and corrected by subtracting the signals of the buffer.

ATR-FTIR Experiments. Solid-phase ATR (attenuated total reflectance)-FTIR was performed on a NEXUS-470 FTIR spectrometer (Nicolet) equipped with a DGTS detector, a ZnSe window and a single-bounce ATR accessory (Nicolet Omni Sampler). The spectra were recorded with a resolution of 4 cm^{-1} and averaged over 256 scans. The data of the peptide were corrected by subtracting the absorption of the related substrates. The derivative analysis was performed by using the OMINC software (Ver. 1.2, Nicolet). Samples were prepared as follows: 100 μL of HBS2 buffer prepared with D_2O was pipetted onto the mica surface or SLBs, and then 30 μL of the peptide solution

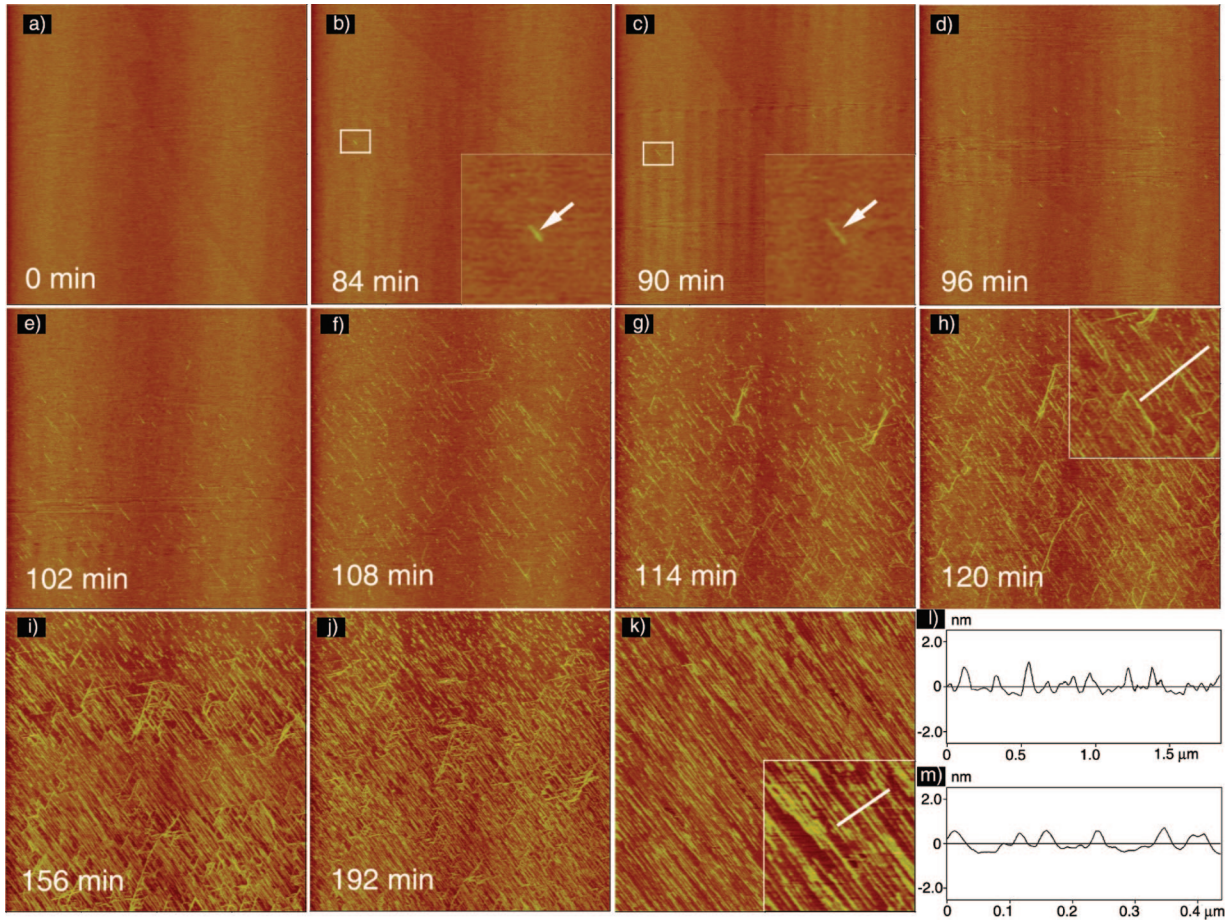

Figure 2. (a−j) Series of snapshots of Aβ_{26-35} fibrogenesis on the POPC SLB within 192 min (image size, 10 × 10 μm; *Z* scale, 5 nm): (a) AFM image of the POPC SLB before the peptide treatment. The insets in b and c are respectively the zoom-in pictures of the corresponding frames indicating the nanofilaments initially formed. (k) The parallel array of the Aβ_{26-35} nanofilaments on the POPC SLB where the growth was not disturbed by the AFM tip (image size, 5 × 5 μm). (l) Section analysis of the inset in picture h. (m) Section analysis of the inset in picture k.

(1.0 mM, dissolved in D_2O) was injected into the droplet for the nanofilaments growth. The formation of the nanofilaments was confirmed by in situ AFM.

Results and Discussion

The peptide Aβ_{26-35} was able to assemble into the homogeneous nanofilaments on the POPC SLBs at a concentration of 50 μM, as observed by solution AFM imaging (Figure 1a). Data analysis shows the average height of the nanofilaments is about 1.0 ± 0.2 nm ($n = 80$), which is close to the height scale of the peptide "lying down" on a surface, presenting a single-sheet structure (Figure 1a). The ATR-FTIR spectrum further shows that the Aβ_{26-35} nanofilaments assembled on the membrane display a strong absorption at about 1627 cm^{-1} and a weak band around 1693 cm^{-1}, the typical characteristics of antiparallel β-sheet[28] (Figure 1b). However, without the presence of the POPC SLB, Aβ_{26-35} displayed random coil conformation[29] and did not show any conformational changes and signs of the fibrogenesis under the same condition (Figure 1c). Recently, Linse's group[30] has reported that nanoparticles are able to enhance the rate of protein fibrogenesis by decreasing the lag time for the nucleation of proteins and the surface effect of increasing the local protein concentration on nanoparticles is achieved by promoting the adherence of protein molecules on the surfaces of nanoparticles. It is possible for the POPC SLB with a zwitterionic surface to facilitate the peptide adsorption onto the membrane surface, increase the local concentration of the peptide at the membrane−water interface by interacting with the positively charged N-terminus of Aβ_{26-35} peptide, and promote the peptide nucleation and the subsequent fibrogenesis.[31]

The dynamic process of Aβ_{26-35} fibrogenesis on the POPC SLB was recorded by in situ AFM at room temperature. A set of representative time-lapse AFM images with an interval of 6 min shows the pivotal stages of the Aβ_{26-35} fibrogenesis (Figure 2a−j). The Aβ_{26-35} fibrogenesis on the POPC SLB underwent a stepwise process: at the first stage, there were no observable changes on the SLB surface after the peptide treatment until a short nanofilament was first observed at 84 min (Figure 2b, inset); afterward, the reaction occurred at a higher rate, and many nanofilaments were formed and extended in length from the nanometer scale to the micrometer scale within a relatively short time of about 30 min (Figure 2c−h); about 120 min later, the fibrogenesis slowed down because of the reduction of the free peptide molecules in solution. This stepwise process is similar to that of the peptide self-assembly in solution, in which the peptide fibrogenesis usually undergoes a slow lag time of nucleation of the peptide molecules and a quick growth phase of the nuclei-based fibrillar growth, as described by the nucleation-dependent polymerization (NDP) model.[32] In a previous study, Terzi et al. reported that, after 10 min of incubation with lipid vesicles, a similar Aβ fragment, Aβ_{25-35}, displays the conformational characteristics of a random coil rather than β-sheet.[33] On the basis of our observation that the

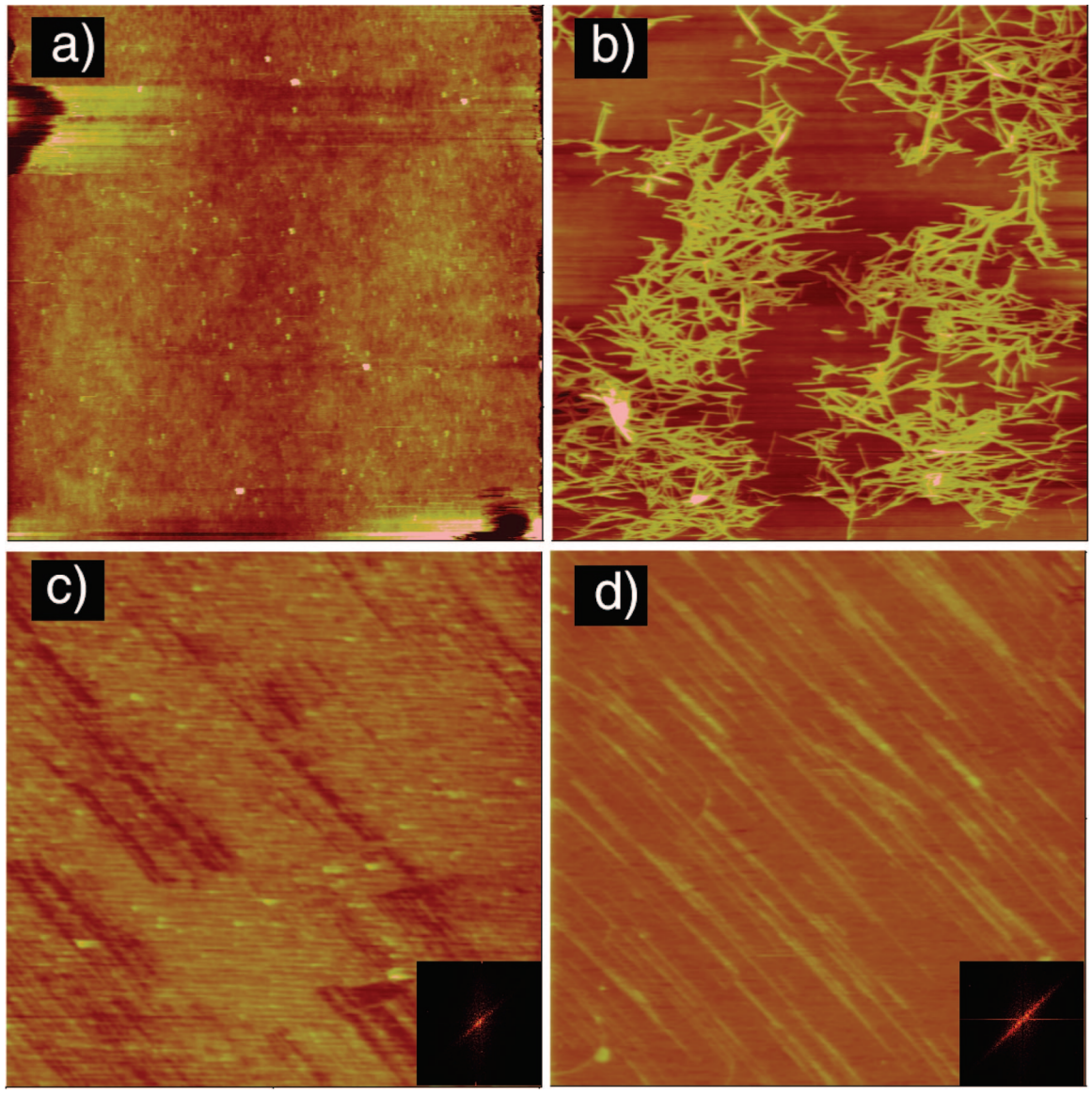

Figure 3. Representative AFM images of the Aβ_{26-35} self-assemblies on the different substrates: (a) negatively charged glass (image size, 10 × 10 μm; *Z* scale, 10 nm); (b) hydrophobic siliconized glass (image size, 10 × 10 μm; *Z* scale, 20 nm); (c) POPC/POPG SLB; (d) POPC/SM SLB (image size, 5 × 5 μm; *Z* scale, 10 nm). The insets in pictures c and d are the Fourier transform analysis.

Aβ_{26-35} fibrogenesis on membranes undergoes a very slow lag phase, we consider that, in those conditions, the interactions between Aβ_{25-35} membranes could be at the initial lag phase of the whole process, and the conformational conversion was not significant at this stage.

In the fibrogenesis process, we found that most of the Aβ_{26-35} nanofilaments tended to align and elongate on the POPC SLBs in a parallel fashion and some of them oriented to other directions (Figure 2). To determine if this oriented growth was caused by AFM scanning, we examined the nanofilaments formed in the fields away from the in situ AFM scanning. Interestingly, we found that the highly ordered parallel-oriented surface pattern was uniformly formed on the whole POPC SLB. A representative image of the parallel array was shown in Figure 2k. Moreover, in different experiments, the orientations of the nanofilaments array are usually different from the directions of AFM tip movement. These observations indicate that the parallel-oriented surface patterns were formed due to the oriented fibrogenesis of Aβ_{26-35} on POPC SLBs rather than the AFM scanning.

The parallel alignments of the one-dimensional nanostructures have been achieved via Langmuir−Blodgett technique[34–36] or by combing the self-assembly with a physical process, such as dewetting[37] and contact-line pinning.[38] However, in our experiments, the self-assembly occurred in wet conditions, and it is almost impossible for the dewetting-caused array to occur. Additionally, the parallel-oriented array of the Aβ_{26-35} nanofilaments was homogeneously formed on the whole membrane, which is much different from that of the dewetting method.[37] To clarify whether or not the parallel-oriented fibrogenesis was attributed to the Aβ_{26-35} structure properties, we investigated the Aβ_{26-35} self-assemblies on the glass slide (negatively charged surface) and siliconized glass slide (hydrophobic surface) that display the amorphous surfaces similar to lipid bilayers. As shown in Figure 3a,b, under the same conditions, Aβ_{26-35} deposited and formed amorphous aggregates on the glass surface and formed thick nanofibrils without any orientation preferences on the siliconized glass surface. These phenomena are much different from the Aβ_{26-35} fibrogenesis on

the lipid membranes, indicating the Aβ_{26-35} structural property is not the determinant for the parallel-oriented pattern formation.

According to the liquid crystalline theory, the POPC bilayers are at the fluid L-alpha phase at room temperature. In contrast to the solid substrates, the lipid molecules can diffuse freely in the membrane plane. We presume that the membrane fluidity allows the adsorbed peptide molecules, nuclei, and nanofilaments to float at the membrane−water interface, which would therefore easily adopt the favorable orientation for self-assembly and present a much different behavior from those of Aβ_{26-35} on the solid substrates. Moreover, as the density increases, it is increasingly difficult for the floating nuclei and nanofilaments to point in random directions under the strains of lowering energy. The floating nuclei and nanofilaments may grow and elongate in a specific direction and form the parallel alignment, which could maximize the entropy of the self-assembled system and stabilize the structure by minimizing the excluded volume per filaments and nuclei in the array.[39] To testify this postulation, we examined the Aβ_{26-35} fibrogenesis on other generally used model membranes, such as POPC/POPG (55:45, w/w) and POPC/SM (50:50, w/w) SLBs (Figure 3c,d). The parallel arrays of the Aβ_{26-35} nanofilaments were formed in these SLBs systems after incubation, suggesting the fluidity of lipid membranes is indispensable for the parallel-oriented fibrogenesis of the Aβ_{26-35} peptide.

Besides, because the lipid POPG is negatively charged, the fibrogenesis of positively charged Aβ_{26-35} was significantly accelerated and formed a nanofilaments array in a high density as comparison with that on POPC bilayers. This phenomenon is very similar to that of Aβ fibrogenesis accelerated by acidic phospholipids, which has been thought to be electrostatically driven.[40] However, the POPC/SM SLB did not bring significant changes in the dynamics of Aβ_{26-35} fibrogenesis. It could be attributed to the SM lipids having the same zwitterionic head in their hydrophilic part as compared to POPC.

The remaining puzzle in exploring the parallel-oriented fibrogenesis is about what ultimately determines the direction of the nanofilaments array on the lipid membranes. We prefer to consider that the direction of the nanofilaments array and growth is stochastic, which is associated with the orientation distributions of the adsorbed molecules and nuclei and is related to the minor disturbance of the lipid membranes during the Aβ_{26-35} fibrogenesis. It may be a possible way to control the direction of the parallel-oriented fibrogenesis by physical methods, such as electromagnetic fields.

Conclusion

In summary, by using in situ AFM, CD, and FTIR, we found that, on the POPC SLBs, the Aβ_{26-35} peptide self-assembled into the highly ordered nanofilaments with an average height of about 1.0 ± 0.2 nm accompanying with the conformational transition from random coil to β-sheet. The Aβ_{26-35} fibrogenesis on the POPC SLBs underwent a stepwise process and formed the highly ordered parallel array of the Aβ_{26-35} nanofilaments on the membranes. The parallel-oriented fibrogenesis of Aβ_{26-35} occurred on different lipid SLBs but not on the solid substrates, suggesting that the fluid nature of lipid membranes is the key cofactor for the parallel-oriented fibrogenesis on lipid membranes. These results provide an insight for further investigation of the surface chemistry of peptide self-assembly on lipid membranes. It also offers a possible way to fabricate supramolecular architectures on the surface of soft materials by using peptide self-assembly.

Acknowledgment. This work was financially supported by NSFC (Grant 20673001 and 20273002).

References and Notes

(1) Zhang, S. G. *Biotechnol. Adv.* **2002**, *20*, 321.
(2) Zhang, S. G. *Nat. Biotechnol.* **2003**, *21*, 1171.
(3) Zhang, S. G.; Gelain, F.; Zhao, X. J. *Seminars Cancer Biol.* **2005**, *15*, 413.
(4) Fairman, R.; Akerfeldt, K. S. *Curr. Opin. Struct. Biol.* **2005**, *15*, 453.
(5) Whitesides, G. M.; Grzybowski, B. *Science* **2002**, *295*, 2418.
(6) Fu, X. Y.; Wang, Y.; Huang, L. X.; Sha, Y. L.; Gui, L. L.; Lai, L. H.; Tang, Y. Q. *Adv. Mater.* **2003**, *15*, 902.
(7) Reches, M.; Gazit, E. *Nat. Nanotechnol.* **2006**, *1*, 195.
(8) Hamley, I. W. *Angew. Chem., Int. Ed.* **2003**, *42*, 1692.
(9) Kovaric, B. C.; Kokona, B.; Schwab, A. D.; Twomey, M. A.; de Paula, J. C.; Fairman, R. *J. Am. Chem. Soc.* **2006**, *128*, 4166.
(10) Wagner, D. E.; Phillips, C. L.; Ali, W. M.; Nybakken, G. E.; Crawford, E. D.; Schwab, A. D.; Smith, W. F.; Fairman, R. *Proc. Natl. Acad. Sci. U.S.A.* **2005**, *102*, 12656.
(11) Ellis-Behnke, R. G.; Liang, Y. X.; You, S. W.; Tay, D. K. C.; Zhang, S. G.; So, K. F.; Schneider, G. E. *Proc. Natl. Acad. Sci. U.S.A.* **2006**, *103*, 5054.
(12) Kisiday, J.; Jin, M.; Kurz, B.; Hung, H.; Semino, C.; Zhang, S.; Grodzinsky, A. J. *Proc. Natl. Acad. Sci. U.S.A.* **2002**, *99*, 9996.
(13) Carrell, R. W.; Lomas, D. A. *Lancet* **1997**, *350*, 134.
(14) Ross, C. A.; Poirier, M. A. *Nat. Rev. Neurosci.* **2004**, S10.
(15) Hoyer, W. G.; Cherny, D.; Subramaniam, V.; Jovin, T. M. *J. Mol. Biol.* **2004**, *340*, 127.
(16) Kowalewski, T.; Holtzman, D. M. *Proc. Natl. Acad. Sci. U.S.A.* **1999**, *96*, 3688.
(17) Whitehouse, C.; Fang, J. Y.; Aggeli, A.; Bell, M.; Brydson, R.; Fishwick, C. W. G.; Henderson, J. R.; Knobler, C. M.; Owens, R. W.; Thomson, N. H.; Smith, D. A.; Boden, N. *Angew. Chem., Int. Ed.* **2005**, *44*, 1965.
(18) Yang, G. C.; Woodhouse, K. A.; Yip, C. M. *J. Am. Chem. Soc.* **2002**, *124*, 10648.
(19) Zhang, F.; Du, H. N.; Zhang, Z. X.; Ji, L. N.; Li, H. T.; Tang, L.; Wang, H. B.; Fan, C. H.; Xu, H. J.; Zhang, Y.; Hu, J.; Hu, H. Y.; He, J. H. *Angew. Chem., Int. Ed.* **2006**, *45*, 3611.
(20) Bokvist, M.; Lindstrom, F.; Watts, A.; Grobner, G. *J. Mol. Biol.* **2004**, *335*, 1039.
(21) Terzi, E.; Holzemann, G.; Seelig, J. *Biochemistry* **1997**, *36*, 14845.
(22) Kellermayer, M. S. Z.; Karsai, A.; Benke, M.; Soos, K.; Penke, B. *Proc. Natl. Acad. Sci. U.S.A.* **2008**, *105*, 141.
(23) Serpell, L. C. *Biochim. Biophys. Acta, Mol. Basis Dis.* **2000**, *1502*, 16.
(24) Fields, G. B.; Noble, R. L. *Int. J. Pept. Protein Res.* **1990**, *35*, 161.
(25) Chiantia, S.; Kahya, N.; Schwille, P. *Langmuir* **2005**, *21*, 6317.
(26) Giocondi, M. C.; Milhiet, P. E.; Dosset, P.; Le Grimellec, C. *Biophys. J.* **2004**, *86*, 861.
(27) Saslowsky, D. E.; Lawrence, J.; Ren, X. Y.; Brown, D. A.; Henderson, R. M.; Edwardson, J. M. *J. Biol. Chem.* **2002**, *277*, 26966.
(28) Miyazawa, T.; Blout, E. R. *J. Am. Chem. Soc.* **1961**, *83*, 712.
(29) Yang, J. T.; Wu, C. S. C.; Martinez, H. M. *Methods Enzymol.* **1986**, *130*, 208.
(30) Linse, S.; Cabaleiro-Lago, C.; Xue, W. F.; Lynch, I.; Lindman, S.; Thulin, E.; Radford, S. E.; Dawson, K. A. *Proc. Natl. Acad. Sci. U.S.A.* **2007**, *104*, 8691.
(31) Gorbenko, G. P.; Kinnunen, P. K. J. *Chem. Phys. Lipids* **2006**, *141*, 72.
(32) Shen, C. L.; Scott, G. L.; Merchant, F.; Murphy, R. M. *Biophys. J.* **1993**, *65*, 2383.
(33) Terzi, E.; Holzemann, G.; Seelig, J. *Biochemistry* **1994**, *33*, 7434.
(34) Yang, P. D. *Nature* **2003**, *425*, 243.
(35) Tao, A.; Kim, F.; Hess, C.; Goldberger, J.; He, R. R.; Sun, Y. G.; Xia, Y. N.; Yang, P. D. *Nano Lett.* **2003**, *3*, 1229.
(36) Whang, D.; Jin, S.; Wu, Y.; Lieber, C. M. *Nano Lett.* **2003**, *3*, 1255.
(37) van Hameren, R.; Schon, P.; vanBuul, A. M.; Hoogboom, J.; Lazarenko, S. V.; Gerritsen, J. W.; Engelkamp, H.; Christianen, P. C. M.; Heus, H. A.; Maan, J. C.; Rasing, T.; Speller, S.; Rowan, A. E.; Elemans, J. A. A. W.; Nolte, R. J. M. *Science* **2006**, *314*, 1433.
(38) Deegan, R. D. *Phys. Rev. E* **2000**, *61*, 475.
(39) Kim, F.; Kwan, S.; Akana, J.; Yang, P. D. *J. Am. Chem. Soc.* **2001**, *123*, 4360.
(40) Aisenbrey, C.; Borowik, T.; Bystrom, R.; Bokvist, M.; Lindstrom, F.; Misiak, H.; Sani, M. A.; Grobner, G. *Eur. Biophys. J.* **2008**, *37*, 247.

JP802424H